

Link prediction via controlling the leading eigenvector

YAN-LI LEE, QIANG DONG and TAO ZHOU^(a)

Complex Lab, University of Electronic Science and Technology of China - Chengdu 611731, PRC

PACS 89.20.Ff – Computer science and technology
 PACS 89.75.Hc – Networks and genealogical trees
 PACS 89.65.-s – Social and economic systems

Abstract – Link prediction is a fundamental challenge in network science. Among various methods, similarity-based algorithms are popular for its simplicity, interpretability, high efficiency and satisfactory performance. In this Letter, we show that the most elementary index, namely the common neighbor (CN) index, is dominated by the leading eigenvector of the adjacency matrix of the target network. Accordingly, we propose a parameter-free algorithm that keeps the contributions of the leading eigenvector and the secondary eigenvector the same. Extensive experiments on real networks demonstrate that the prediction performance of the proposed algorithm is remarkably better than well-performed local similarity indices in the literature. A further proposed algorithm that can adjust the contribution of leading eigenvector shows the superiority over state-of-the-art global algorithms for both higher accuracy and lower computational complexity.

Introduction. – The booming of network science has brought about a new vision to explore and tackle problems existed in biology [1–3], economics [4–7], social science [8], data science [9, 10] and so on. As an increasing number of datasets are structured by networks (e.g., protein-protein interaction networks, miRNA-disease association networks, drug-target networks, user-product networks, company investment networks, collaboration networks, citation networks, etc.), link prediction [9, 11] has found wide applications in many scenarios. For example, in laboratorial experiments, instead of blindly check all possible interactions among proteins, predicting potential interactions based on existed interactions can sharply reduce the experimental costs if the prediction performance is accurate enough [12]. In social website, academic website and e-commerce platform, a good recommendation of friends, citations, collaborators and products can enhance the loyalties and experience of users and the conversion rate in trading platform [7]. In addition, link prediction is also helpful in probing network evolution mechanisms [13, 14] and estimating the extent of regularity of the network formation [15, 16]. In a word, link prediction is a significant and challenging problem in network science.

Various methods are proposed, including similarity-based algorithms [17–19], probabilistic models [20, 21], maximum likelihood methods [22–24], network embedding

[25–27] and other representatives [28–30]. Among them, similarity-based algorithms are popular for its simplicity, interpretability, high efficiency and satisfactory performance. In this Letter, we show that the most elementary index, namely the common neighbor (CN) index [17], is dominated by the leading eigenvector of the adjacency matrix \mathbf{A} of the target network. That results from the huge gap between the largest eigenvalue and the second largest eigenvalue in many real networks [31]. We propose a parameter-free algorithm that adopts a recently proposed enhancement framework for local similarity indices [32] and keeps the contributions of the leading eigenvector and the secondary eigenvector the same. This algorithm is abbreviated as CLE because its underlying idea is controlling the leading eigenvector. Extensive experiments on real networks demonstrate that the prediction performance of CLE is remarkably better than well-performed local similarity indices and their enhanced versions. We further propose a parameter-dependent algorithm with adjustable contribution of the leading eigenvector, which outperforms elaborately designed global algorithms.

Methods. – The CN index directly counts the number of common neighbors between two nodes, as

$$S_{xy}^{CN} = |\Gamma_x \cap \Gamma_y|, \quad (1)$$

where x and y are two arbitrary nodes and Γ_x is the set of neighbors of x . The CN matrix \mathbf{S}^{CN} can be decomposed

^(a)E-mail: zhutou@ustc.edu

as

$$\mathbf{S}^{CN} = \mathbf{A}^2 = \sum_{d=1}^N \lambda_d^2 \mathbf{v}_d \mathbf{v}_d^T = \sum_{d=1}^N \lambda_d^2 \mathbf{S}^{(d)}, \quad (2)$$

where N is the number of nodes, λ_d and \mathbf{v}_d are the d th eigenvalue and the corresponding orthogonal and normalized eigenvector of \mathbf{A} , and $\lambda_1^2 \geq \lambda_2^2 \geq \dots \geq \lambda_N^2$. Notice that, node x can be represented by the N eigenvectors as

$$\mathbf{w}_x = [\lambda_1 v_{1x}, \lambda_2 v_{2x}, \dots, \lambda_N v_{Nx}], \quad (3)$$

where v_{dx} is the x th element of the d th eigenvector. Then, \mathbf{S}_{xy}^{CN} is the dot product of \mathbf{w}_x and \mathbf{w}_y , as

$$\mathbf{S}_{xy}^{CN} = |\Gamma_x \cap \Gamma_y| = \mathbf{w}_x \mathbf{w}_y^T = \sum_{d=1}^N \lambda_d^2 v_{dx} v_{dy}. \quad (4)$$

Accordingly, the contribution of each eigenvector to CN is proportional to the square of its eigenvalue. Therefore, the gap between λ_1^2 and λ_2^2 for many real networks [31] leads to the dominant contribution of the leading eigenvector. Take the email communication network DNC [33] as an example (the detailed description is shown later), λ_1^2 of DNC is 2.13 times larger than λ_2^2 . As a result, the Pearson correlation coefficient r between \mathbf{S}^{CN} and $\mathbf{S}^{(1)}$ is much higher than coefficients between \mathbf{S}^{CN} and others (see fig. 1).

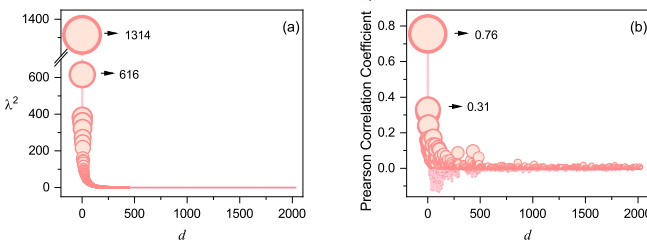


Fig. 1: The dominant role of the leading eigenvector on DNC. (a) The distribution of λ^2 and (b) the Pearson correlation coefficient r between \mathbf{S}^{CN} and $\mathbf{S}^{(d)}$. The size of the circle is proportional to the corresponding value in y -axis.

The dominant role of the leading eigenvector may over-suppress useful information contained in other eigenvectors, and thus to depress the contribution of the leading eigenvector may better characterize the node similarity. The most straightforward way to tackle this problem is to make the contribution of $\mathbf{S}^{(1)}$ the same as $\mathbf{S}^{(2)}$. Accordingly, a parameter-free similarity matrix can be obtained as

$$\tilde{\mathbf{S}} = \lambda_2^2 \mathbf{S}^{(1)} + \sum_{d=2}^N \lambda_d^2 \mathbf{S}^{(d)}. \quad (5)$$

It is natural to extend $\tilde{\mathbf{S}}$ to a parameter-dependent similarity matrix as

$$\tilde{\mathbf{S}}^* = \alpha \lambda_1^2 \mathbf{S}^{(1)} + \sum_{d=2}^N \lambda_d^2 \mathbf{S}^{(d)}, \quad (6)$$

where α is a tunable parameter controlling the contribution of \mathbf{v}_1 .

Very recently, an enhancement framework, named self-included collaborative filtering (SCF), is proposed for local similarity indices [32]. Given a similarity matrix \mathbf{S} , the SCF-enhanced matrix reads

$$\ddot{\mathbf{S}} = (\mathbf{A} + \mathbf{I})\mathbf{S} + [(\mathbf{A} + \mathbf{I})\mathbf{S}]^T, \quad (7)$$

where \mathbf{I} is the identity matrix. This framework largely improves the prediction performance and the robustness of local similarity indices. By applying the enhancement framework on $\tilde{\mathbf{S}}$ and $\tilde{\mathbf{S}}^*$, we can obtain a parameter-free algorithm (CLE) as

$$\mathbf{S}^{CLE} = (\mathbf{A} + \mathbf{I})\tilde{\mathbf{S}} + [(\mathbf{A} + \mathbf{I})\tilde{\mathbf{S}}]^T \quad (8)$$

and a parameter-dependent algorithm (CLE*) as

$$\mathbf{S}^{CLE*} = (\mathbf{A} + \mathbf{I})\tilde{\mathbf{S}}^* + [(\mathbf{A} + \mathbf{I})\tilde{\mathbf{S}}^*]^T. \quad (9)$$

Clearly, CLE* reduces to CLE when $\alpha = \lambda_2^2/\lambda_1^2$, and to $\ddot{\mathbf{S}}^{CN}$ when $\alpha = 1$ ($\ddot{\mathbf{S}}^{CN}$ is the SCF-enhanced CN index).

Results. – To test the algorithmic performance, 18 networks from disparate fields are considered, including (1) FWF [36]—the predator-prey network of animals in ecosystem of Coastal bay in Florida Bay in the dry season; (2) FWE [36]—the predator-prey network of animals in Everglades Graminoids in the west season; (3) RAD [33]—the email communication network between employees of a mid-sized manufacturing company; (4) DNC [33]—the email communication network in the 2016 Democratic Committee email leak; (5) HFR [33]—the friendship network among users of the website *hamsterster.com*; (6) HG [33]—the human contact network measured by carried wireless devices; (7) WR [37]—the religious social network where each link denotes a follower-followee relationship in *Weibo*; (8) PH [33]—the innovation spreading network in which nodes denote physicians and links denote friendships or discussions between physicians; (9) MR [38]—the rating network where links denote ratings of users to movies; (10) BG [33]—the hyperlink network among blogs in the context of the 2004 US election; (11) GFA [34]—the gene functional association network of *C.elegans*; (12) BM13 [39]—the protein-protein interaction network in Lit-BM-13; (13) FG [33]—the protein-protein interaction network in *Homo sapiens*; (14) FTB [40]—the trading network of players of 35 national soccer teams; (15) WTN [41]—the world trading network of miscellaneous manufactures of metal among 80 countries in 1994; (16) UST [33]—the air transportation network of US; (17) ATC [33]—the network of airports or service centers, where each link denotes a preferred route between two nodes; (18) ER [33]—the international E-road network between cities in Europe where each link denotes a road between two cities. In the above networks, multiple links and self-connections are not allowed, and directions and weights of links are ignored. The elementary statistics are shown in table 1.

Table 1: Structural statistics of the 18 real networks. N and M are the number of nodes and links. ρ , $\langle k \rangle$, $\langle c \rangle$, $\langle l \rangle$ and σ are the network density, average degree, average clustering coefficient [34], average shortest path length, and assortativity coefficient [35], respectively. $\delta = \lambda_2^2/\lambda_1^2$ measures the eigenvalue gap.

Network	N	M	ρ	$\langle k \rangle$	$\langle c \rangle$	$\langle l \rangle$	σ	δ
FWF	128	2106	0.259	32.91	0.33	1.77	-0.10	0.267
FWE	69	880	0.375	25.51	0.55	1.64	-0.27	0.195
RAD	167	3250	0.234	38.92	0.59	1.97	-0.30	0.086
DNC	2029	4384	0.002	4.32	0.22	3.37	-0.31	0.468
HFR	1858	12534	0.007	13.49	0.14	3.45	-0.09	0.283
HG	274	2124	0.057	15.50	0.63	2.42	-0.47	0.075
WR	6875	64712	0.003	18.83	0.30	3.49	-0.24	0.544
PH	241	923	0.068	7.66	0.22	2.59	-0.08	0.992
MR	1682	94834	0.067	112.76	0.36	2.16	-0.19	0.118
BG	1224	16715	0.022	27.31	0.32	2.74	-0.22	0.655
GFA	297	2148	0.046	14.04	0.29	2.45	-0.16	0.342
BM13	3391	4388	0.001	2.59	0.07	6.61	-0.02	0.895
FG	2239	6432	0.003	5.75	0.04	3.84	-0.33	0.910
FTB	35	118	0.193	6.74	0.27	2.13	-0.26	0.352
WTN	80	875	0.277	21.88	0.75	1.72	-0.39	0.184
UST	332	2126	0.039	12.81	0.62	2.74	-0.21	0.176
ATC	1266	2408	0.003	3.93	0.07	5.93	-0.02	0.723
ER	1174	1417	0.002	2.41	0.02	18.40	0.09	0.955

Consider a network $G(V, E)$ with V the set of nodes and E the set of links. To evaluate the algorithmic performance, E is randomly divided into two parts: the training set E^T contains the known topology, and the testing set E^P is treated as missing links that cannot be used in the prediction. Obviously, $E^T \cup E^P = E$ and $E^T \cap E^P = \emptyset$. Many link prediction algorithms will assign a score to each link and the top- L links (i.e., the L links with highest scores) are the predicted links. AUC, AUPR, precision and recall are the most commonly used metrics to evaluate the link prediction algorithms [11]. Among them, AUC is particularly suitable for link prediction since link prediction is a typical imbalance learning problem with missing links being much fewer than nonexistent links [42]. In addition, AUC is highly interpretable as the value can be understood as the probability that a randomly chosen missing link is assigned a higher score than a randomly chosen nonexistent link. Precision and recall are threshold-dependent metrics, sensitive to the threshold value L . AUPR considers all the precision-recall pairs under different L , which is time-consuming and less interpretable [11]. Thus, we choose AUC as the evaluation metric in this Letter. To calculate the AUC, we randomly select n pairs of links respectively from E^P and $U - E$, where U is the universal set containing all the $N(N-1)/2$ potential links. If there are n_1 times the missing link has higher score and n_2 times the missing link has the same score with the nonexistent link, the corresponding AUC is $(n_1 + 0.5n_2)/n$. If all scores of the candidate links are randomly generated from an independent and identical distribution, the AUC value should be 0.5, and the value exceeds 0.5 indicates the extent that the considered algorithm outperforms the pure chance.

Eight parameter-free local similarity indices are used

to compare with CLE, including the CN index [17], the Adamic-Adar (AA) index [43], the resource allocation (RA) index [18], the CRA index [19] and their SCF-enhanced versions. AA differentiates the role of common neighbors by depressing the contributions of large-degree nodes, as

$$S_{xy}^{AA} = \sum_{z \in \Gamma_x \cap \Gamma_y} \frac{1}{\log k_z}, \quad (10)$$

where k_z is the degree of node z . RA quantifies node similarity by a resource allocation process [44], where each neighbor of x allocates one unit resource equally to its neighbors, and the similarity of x and y is the resource that y receives from x , namely

$$S_{xy}^{RA} = \sum_{z \in \Gamma_x \cap \Gamma_y} \frac{1}{k_z}. \quad (11)$$

CRA prefers node pairs with common neighbors densely connected [19], as

$$S_{xy}^{CRA} = \sum_{z \in \Gamma_x \cap \Gamma_y} \frac{\gamma_z}{k_z}, \quad (12)$$

where $\gamma_z = |\Gamma_z \cap \Gamma_x \cap \Gamma_y|$. The enhanced versions of CN, AA, RA and CRA (i.e., \tilde{S}^{CN} , \tilde{S}^{AA} , \tilde{S}^{RA} and \tilde{S}^{CRA}) can be obtained by eq. (7).

The prediction performance of the 9 indices are reported in table 2. According to the winning rate R of each index on 14 real networks and the average AUC values, CLE is remarkably better than all other indices and achieves significant improvement compared with \tilde{S}^{CN} by controlling the contribution of \mathbf{v}_1 . The relatively poor performance of CRA category may results from few local community links in some networks.

Table 2: AUC of CLE and the 8 benchmark indices on 18 real networks. Each result is averaged over 100 independent runs with E^P containing 10% links. The best-performed result for each network, the highest winning rate R and the highest average AUC value are emphasized in bold.

Network	CLE	$\bar{\mathbf{S}}^{CN}$	$\bar{\mathbf{S}}^{AA}$	$\bar{\mathbf{S}}^{RA}$	$\bar{\mathbf{S}}^{CRA}$	\mathbf{S}^{CN}	\mathbf{S}^{AA}	\mathbf{S}^{RA}	\mathbf{S}^{CRA}
FWF	0.910	0.817	0.817	0.830	0.848	0.605	0.601	0.608	0.637
FWE	0.922	0.846	0.849	0.861	0.889	0.676	0.688	0.692	0.706
RAD	0.941	0.909	0.911	0.915	0.887	0.913	0.913	0.917	0.917
DNC	0.848	0.790	0.790	0.792	0.770	0.800	0.800	0.805	0.749
HFR	0.952	0.935	0.945	0.955	0.910	0.805	0.807	0.807	0.652
HG	0.950	0.932	0.934	0.935	0.904	0.932	0.932	0.933	0.925
WR	0.974	0.964	0.965	0.969	0.954	0.925	0.928	0.929	0.871
PH	0.901	0.908	0.907	0.910	0.769	0.845	0.841	0.842	0.658
MR	0.943	0.920	0.920	0.925	0.922	0.904	0.904	0.903	0.906
BG	0.940	0.931	0.934	0.940	0.923	0.919	0.921	0.922	0.896
GFA	0.898	0.850	0.868	0.883	0.825	0.848	0.867	0.871	0.764
BM13	0.721	0.684	0.684	0.684	0.538	0.591	0.592	0.589	0.515
FG	0.906	0.852	0.858	0.857	0.697	0.550	0.554	0.556	0.510
FTB	0.807	0.749	0.776	0.774	0.750	0.650	0.653	0.631	0.669
WTN	0.926	0.879	0.885	0.896	0.837	0.858	0.876	0.898	0.891
UST	0.944	0.902	0.911	0.930	0.879	0.932	0.947	0.952	0.919
ATC	0.756	0.715	0.716	0.718	0.530	0.611	0.613	0.609	0.509
ER	0.554	0.551	0.552	0.554	0.500	0.526	0.523	0.524	0.500
R	83.3%	0.0%	0.0%	11.1%	0.0%	0.0%	0.0%	5.6%	0.0%
$\langle AUC \rangle$	0.877	0.841	0.846	0.852	0.796	0.772	0.776	0.777	0.733

To be fair, we compare CLE* with three parameter-dependent benchmarks, including the Katz index [45], the local path (LP) index [46] and the linear optimization (LO) algorithm [47]. Katz considers all paths with exponentially damped contributions along with their lengths, as

$$\mathbf{S}_{xy}^{Katz} = \beta(\mathbf{A})_{xy} + \beta^2(\mathbf{A}^2)_{xy} + \beta^3(\mathbf{A}^3)_{xy} + \dots, \quad (13)$$

where β is a tunable parameter. To avoid the degeneracy of states in CN and make similarities more distinguishable, LP considers both contributions from 2-hop and 3-hop paths, as

$$\mathbf{S}_{xy}^{LP} = (\mathbf{A}^2)_{xy} + \epsilon(\mathbf{A}^3)_{xy}, \quad (14)$$

where ϵ is a tunable parameter. LO assumes that the existence likelihood of a link is a linear summation of contributions of all its neighbors. By solving a corresponding optimization function, the analytical expression of the predicted matrix (can be treated as a similarity matrix) is

$$\mathbf{S}^{LO} = \mathbf{A}\mathbf{Z}^* = \alpha\mathbf{A}(\alpha\mathbf{A}^T\mathbf{A} + \mathbf{I})^{-1}\mathbf{A}^T\mathbf{A}, \quad (15)$$

where α is a free parameter.

The AUC values of CLE* and the three compared algorithms are reported in table 3. Most strikingly, CLE* outperforms all others including the global algorithm LO, which is known to be one of the most accurate algorithms thus far.

Analyses. – We first test the robustness of the considered algorithms against the data sparsity by varying the size of the training set from 50% to 95%. Figure 2

Table 3: AUC of CLE* and the three parameter-dependent benchmarks on 18 real networks. Parameters are tuned to their optimal values corresponding to highest AUC values. Each result is averaged over 100 independent runs with E^P containing 10% links. The best-performed result for each network, the highest winning rate R and the highest average AUC value are emphasized in bold.

Network	CLE*	\mathbf{S}^{LO}	\mathbf{S}^{LP}	\mathbf{S}^{Katz}
FWF	0.920	0.950	0.812	0.718
FWE	0.924	0.941	0.842	0.788
RAD	0.941	0.942	0.910	0.911
DNC	0.849	0.838	0.797	0.739
HFR	0.953	0.954	0.936	0.914
HG	0.957	0.947	0.934	0.925
WR	0.974	0.971	0.964	0.952
PH	0.905	0.887	0.913	0.922
MR	0.944	0.950	0.923	0.908
BG	0.940	0.946	0.932	0.928
GFA	0.901	0.895	0.871	0.867
BM13	0.727	0.638	0.685	0.644
FG	0.915	0.898	0.852	0.752
FTB	0.786	0.787	0.764	0.692
WTN	0.928	0.924	0.882	0.876
UST	0.948	0.938	0.942	0.925
ATC	0.760	0.615	0.717	0.755
ER	0.566	0.505	0.557	0.633
R	50.0%	38.9%	0.0%	11.1%
$\langle AUC \rangle$	0.880	0.863	0.846	0.825

(a) shows an example on DNC. CLE and CLE* are relatively insensitive to the data sparsity and always perform best. In contrast, the CN-based indices (i.e., CN, AA, RA and CRA) perform much worse when training sets contain fewer links. That is because the common neighbor

based indices depend on the clustering of networks and the CRA category indices depend on the local community links. The increasing of the links in E^P will reduce the clustering coefficient and the local community links for training networks. Figure 2 (b) further shows the average AUC values over the 18 real networks with the ratios of training set being 50% and 90%, respectively. Similar to the DNC example, CLE* performs overall best.

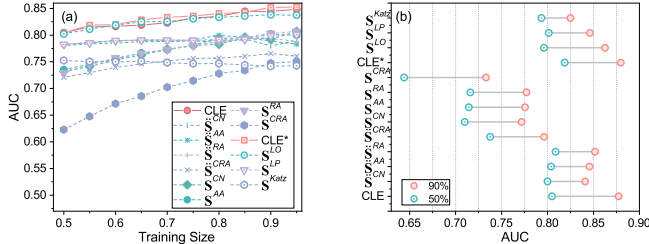


Fig. 2: The robustness of CLE and CLE* against the data sparsity. (a) AUC of the 13 algorithms for different training sizes on DNC. (b) The average AUC values over the 18 real networks for the 13 algorithms, where the ratios of training set are 50% and 90%. The results are averaged over 100 independent runs.

Next, we analyze the time complexity of the considered algorithms. To calculate CN, AA and RA, for each node x , we first search its neighbors, and then search the neighbors of each of x 's neighbors, so that all 2-hop paths are taken into account. Therefore, the time complexity of \mathbf{S}^{CN} , \mathbf{S}^{AA} and \mathbf{S}^{RA} is $O(N \langle k \rangle^2)$. The time complexity of \mathbf{S}^{CRA} , $\tilde{\mathbf{S}}^{CN}$, $\tilde{\mathbf{S}}^{AA}$, $\tilde{\mathbf{S}}^{RA}$ and \mathbf{S}^{LP} is $O(N \langle k \rangle^3)$ since one more search is required. Analogously, the time complexity of $\tilde{\mathbf{S}}^{CRA}$ is $O(N \langle k \rangle^4)$. The time complexity of \mathbf{S}^{Katz} and \mathbf{S}^{LO} is $O(N^3)$, dominated by the matrix inversion operator. Direct spectral decomposition in CLE and CLE* is time-consuming, instead we can rewrite $\tilde{\mathbf{S}}$ and $\tilde{\mathbf{S}}^*$ as

$$\tilde{\mathbf{S}} = \mathbf{A}^2 + (\lambda_2^2 - \lambda_1^2)\mathbf{S}^{(1)} \quad (16)$$

and

$$\tilde{\mathbf{S}}^* = \mathbf{A}^2 + (\alpha - 1)\lambda_1^2\mathbf{S}^{(1)}. \quad (17)$$

As a result, the time consumption of CLE and CLE* mainly comes from the calculation of the leading eigenvector, the largest eigenvalue and the second largest eigenvalue, which can be quickly obtained by the Lanczos method through repeated matrix-vector multiplication [48]. Therefore, the time complexity of CLE and CLE* is $O(N^2)$. We also report the CPU times of the 13 algorithms in fig. 3. Overall speaking, CLE and CLE* achieve the best prediction performance, while require much shorter CPU time than global algorithms.

We finally compare the parameter-free algorithm CLE and the parameter-dependent algorithm CLE*. To our surprise, CLE is highly competitive with CLE* on all the considered networks. Taking DNC as a typical example, as shown in fig. 4(a), the AUC of CLE is very close to the optimal AUC for CLE*, while the AUC of $\tilde{\mathbf{S}}^{CN}$ is much lower. Figure 4(b) compares the AUC values of CLE and

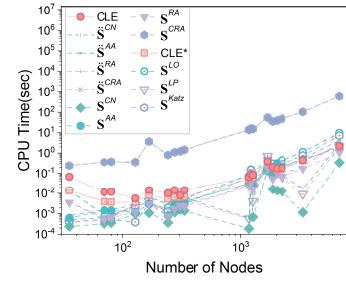


Fig. 3: CPU times of different algorithms with varying network sizes. The 18 data points for each algorithm correspond to the 18 real networks. All computations are implemented on a desktop computer with a single Intel(R) Core (TM) processor (3.40 GHZ). Results for CLE and CLE* are marked in red.

CLE* on all 18 real networks. It is observed that almost all the points are located on the diagonal line with the mean difference between their AUC values being only 0.0025. The Mann-Whitney U Test [49] also suggests that there is no significant difference between their AUC values (p -value > 0.05).

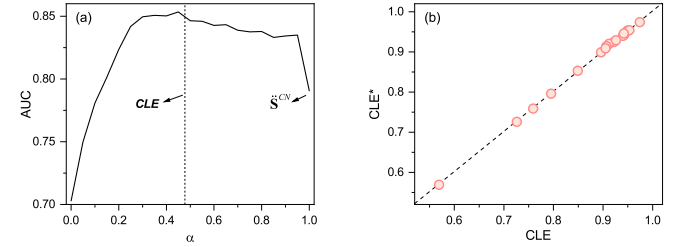


Fig. 4: Comparison of CLE and CLE*. (a) AUC of CLE* versus α for DNC. (b) The relation of AUC between CLE and CLE* on 18 real networks, where each data point is averaged over 100 independent runs with E^P containing 10% links. CLE is marked by dash line, and $\tilde{\mathbf{S}}^{CN}$ corresponds to $\alpha = 1$.

Conclusion. — This Letter proposes two algorithms, CLE (parameter-free) and CLE* (parameter-dependent), by controlling the leading eigenvector of the adjacency network \mathbf{A} . Experiments on 18 real networks show the following three main findings. (i) CLE outperforms the classical local similarity indices and their enhanced versions. (ii) CLE* outperforms the state-of-the-art global algorithms. (iii) The prediction performance of CLE and CLE* is highly competitive. In addition to the high prediction accuracy, CLE and CLE* have lower time complexity than many known global algorithms and thus can be applied at least to mid-sized networks.

This work was partially supported by the National Natural Science Foundation of China (Grant Nos. 11975071 and 61673086), the Science Strength Promotion Program of UESTC under Grant No. Y03111023901014006,

and the Fundamental Research Funds for the Central Universities under Grant No. ZYGX2016J196.

REFERENCES

- [1] GOSAK M., MARKOVIĆ R., DOLENŠEK J., RUPNIK M. S., MARHL M., STOŽER A. and PERC M., *Phys. Life Rev.*, **24** (2018) 118.
- [2] BARABÁSI A.-L., GULBAHCE N. and LOSCALZO J., *Nat. Rev. Genet.*, **12** (2011) 56.
- [3] BARABÁSI A.-L. and OLTVAI Z. N., *Nat. Rev. Genet.*, **5** (2004) 101.
- [4] JACKSON M. O., *J. Econ. Perspect.*, **28** (2014) 3.
- [5] SCHWEITZER F., FAGIOLI G., SORNETTE D., VEGA-REDONDO F., VESPIGNANI A. and WHITE D. R., *Science*, **325** (2009) 422.
- [6] GAO J., ZHANG Y.-C. and ZHOU T., *Phys. Rep.*, **817** (2019) 1.
- [7] LÜ L., MEDO M., YEUNG C. H., ZHANG Y.-C., ZHANG Z.-K. and ZHOU T., *Phys. Rep.*, **519** (2012) 1.
- [8] KOSSINETS G. and WATTS D. J., *Science*, **311** (2006) 88.
- [9] LÜ L. and ZHOU T., *Physica A*, **390** (2011) 1150.
- [10] ZANIN M., PAPO D., SOUSA P. A., MENASALVAS E., NICCHI A., KUBIK E. and BOCCALETTI S., *Phys. Rep.*, **635** (2016) 1.
- [11] ZHOU T., *arXiv:2102.11472*, (2021) .
- [12] DING H., TAKIGAWA I., MAMITSUKA H. and ZHU S., *Briefings Bioinf.*, **15** (2013) 734.
- [13] WANG W.-Q., ZHANG Q.-M. and ZHOU T., *EPL*, **98** (2012) 28004.
- [14] ZHANG Q.-M., XU X.-K., ZHU Y.-X. and ZHOU T., *Sci. Rep.*, **5** (2015) 10350.
- [15] LÜ L., PAN L., ZHOU T., ZHANG Y.-C. and STANLEY H. E., *Proc. Natl. Acad. Sci. U.S.A.*, **112** (2015) 2325.
- [16] XIAN X., WU T., QIAO S., WANG X.-Z., WANG W. and LIU Y., *Knowl. Based Syst.*, **196** (2020) 105800.
- [17] LIBEN-NOWELL D. and KLEINBERG J., *J. Am. Soc. Inf. Sci. Technol.*, **58** (2007) 1019.
- [18] ZHOU T., LÜ L. and ZHANG Y.-C., *Eur. Phys. J. B*, **71** (2009) 623.
- [19] CANNISTRACI C. V., ALANIS-LOBATO G. and RAVASI T., *Sci. Rep.*, **3** (2013) 1613.
- [20] NEVILLE J. and JENSEN D., *J. Mach. Learn. Res.*, **8** (2007) 653.
- [21] YU K., CHU W., YU S., TRESP V. and XU Z., *Stochastic relational models for discriminative link prediction*, in *Proceedings of the 19th International Conference on Neural Information Processing Systems* (MIT Press, Cambridge) 2007, pp. 1553–1560.
- [22] CLAUSET A., MOORE C. and NEWMAN M. E. J., *Nature*, **453** (2008) 98.
- [23] GUIMERÀ R. and SALES-PARDO M., *Proc. Natl. Acad. Sci. U.S.A.*, **106** (2009) 22073.
- [24] PAN L., ZHOU T., LÜ L. and HU C.-K., *Sci. Rep.*, **6** (2016) 22955.
- [25] GROVER A. and LESKOVEC J., *Node2vec: Scalable feature learning for networks*, in *Proceedings of the 22nd ACM SIGKDD International Conference on Knowledge Discovery and Data Mining* (ACM Press, New York) 2016, pp. 855–864.
- [26] TANG J., QU M., WANG M., ZHANG M., YAN J. and MEI Q., *Line: Large-scale information network embedding*, in *Proceedings of the 24th International Conference on World Wide Web* (ACM Press, New York) 2015, pp. 1067–1077.
- [27] WANG D., CUI P. and ZHU W., *Structural deep network embedding*, in *Proceedings of the 22nd ACM SIGKDD International Conference on Knowledge Discovery and Data Mining* (ACM Press, New York) 2016, pp. 1225–1234.
- [28] PECH R., HAO D., PAN L., CHENG H. and ZHOU T., *EPL*, **117** (2017) 38002.
- [29] BENSON A. R., ABEBE R., SCHAUER M. T., JADBABAIE A. and KLEINBERG J., *Proc. Natl. Acad. Sci. U.S.A.*, **115** (2018) E11221.
- [30] GHASEMIAN A., HOSSEINMARDI H., GALSTYAN A., AIROLDI E. M. and CLAUSET A., *Proc. Natl. Acad. Sci. U.S.A.*, **117** (2020) 23393.
- [31] FARKAS I. J., DERÉNYI I., BARABÁSI A.-L. and VICSEK T., *Phys. Rev. E*, **64** (2001) 026704.
- [32] LEE Y.-L. and ZHOU T., *arXiv:2103.09907*, (2021) .
- [33] KUNEGIS J., *Konect: the koblenz network collection*, in *Proceedings of the 22nd International Conference on World Wide Web* (ACM Press, New York) 2013, pp. 1343–1350.
- [34] WATTS D. J. and STROGATZ S. H., *Nature*, **393** (1998) 440.
- [35] NEWMAN M. E. J., *Phys. Rev. Lett.*, **89** (2002) 208701.
- [36] ROSSI R. and AHMED N., *The network data repository with interactive graph analytics and visualization*, in *Proceedings of the 29 th AAAI Conference on Artificial Intelligence* (AAAI Press, California) 2015, pp. 4292–4293.
- [37] HU J., ZHANG Q.-M. and ZHOU T., *EPJ Data Sci.*, **8** (2019) 6.
- [38] GROUPLENS, *Movielens datasets*, <http://www.grouplens.org/node/73> (2006).
- [39] KOVÁCS I. A., LUCK K., SPIROHN K., WANG Y., POLLIS C., SCHLABACH S., BIAN W., KIM D.-K., KISHORE N., HAO T. *et al.*, *Nat. commun.*, **10** (2019) 1240.
- [40] BATAGELJ V. and MRVAR A., *Pajek datasets website*, <http://vlado.fmf.uni-lj.si/pub/networks/data/> (2006).
- [41] DOHLEMAN B., *Psychometrika*, **71** (2011) 605.
- [42] LICHTENWALTER R. N., LUSSIER J. T. and CHAWLA N. V., *New perspectives and methods in link prediction*, in *Proceedings of the 16th ACM SIGKDD International Conference on Knowledge Discovery and Data Mining* (ACM Press, New York) 2010, pp. 243–252.
- [43] ADAMIC L. A. and ADAR E., *Soc. Netw.*, **25** (2003) 211.
- [44] OU Q., JIN Y.-D., ZHOU T., WANG B.-H. and YIN B.-Q., *Phys. Rev. E*, **75** (2007) 021102.
- [45] KATZ L., *Psychometrika*, **18** (1953) 39.
- [46] LÜ L., JIN C.-H. and ZHOU T., *Phys. Rev. E*, **80** (2009) 046122.
- [47] PECH R., HAO D., LEE Y.-L., YUAN Y. and ZHOU T., *Physica A*, **528** (2019) 121319.
- [48] CALVETTI D., REICHEL L. and SORENSEN D. C., *Electron. Trans. Numer. Anal.*, **2** (1994) 1.
- [49] MANN H. B. and WHITNEY D. R., *Annals. Math. Stat.*, **18** (1947) 50.

